Journal of
Composites Science

MDPI

Review

Green Reduction of Graphene Oxide Involving Extracts of Plants from Different Taxonomy Groups

Dharshini Perumal [1], Emmellie Laura Albert [2] and Che Azurahanim Che Abdullah [1,2,3,*]

[1] Biophysics Laboratory, Department of Physics, Faculty of Science, Universiti Putra Malaysia, Serdang 43400, Selangor, Malaysia; gs49789@student.upm.edu.my
[2] Nanomaterial Synthesis and Characterization Laboratory, Institute of Nanoscience and Nanotechnology, Universiti Putra Malaysia, Serdang 43400, Selangor, Malaysia; gs51884@student.upm.edu.my
[3] UPM-MAKNA Cancer Research Laboratory, Institute of Bioscience, Universiti Putra Malaysia, Serdang 43400, Selangor, Malaysia
* Correspondence: azurahanim@upm.edu.my; Tel.: +603-9769-6675

Abstract: Graphene, a remarkable material, is ideal for numerous applications due to its thin and lightweight design. The synthesis of high-quality graphene in a cost-effective and environmentally friendly manner continues to be a significant challenge. Chemical reduction is considered the most advantageous method for preparing reduced graphene oxide (rGO). However, this process necessitates the use of toxic and harmful substances, which can have a detrimental effect on the environment and human health. Thus, to accomplish the objective, the green synthesis principle has prompted researchers worldwide to develop a simple method for the green reduction of graphene oxide (GO), which is readily accessible, sustainable, economical, renewable, and environmentally friendly. For example, the use of natural materials such as plants is generally considered safe. Furthermore, plants contain reducing and capping agents. The current review focuses on the discovery and application of rGO synthesis using extracts from different plant parts. The review aims to aid current and future researchers in searching for a novel plant extract that acts as a reductant in the green synthesis of rGO, as well as its potential application in a variety of industries.

Keywords: green synthesis; plant extract; reduced graphene oxide; applications; graphene oxide

Citation: Perumal, D.; Albert, E.L.; Abdullah, C.A.C. Green Reduction of Graphene Oxide Involving Extracts of Plants from Different Taxonomy Groups. *J. Compos. Sci.* **2022**, *6*, 58. https://doi.org/10.3390/jcs6020058

Academic Editor: Francesco Tornabene

Received: 29 October 2021
Accepted: 7 December 2021
Published: 15 February 2022

1. Introduction

Since its discovery in 2004, graphene, a two-dimensional (2D) carbon atom bonded through sp^2 hybridization, has received widespread recognition due to its superior electrical, thermal, mechanical, and optical properties [1,2]. These unique properties mean that graphene has been used in a variety of applications, including biosensors [3], drug delivery [4], solar cells [5], touch panels [6], anti-bacterial activities [7], and the photocatalytic degradation of pollutants [8]. Graphene has been synthesized using various techniques in recent years, including ultrasonic exfoliation, chemical vapor deposition, micro-mechanical exfoliation, epitaxial growth, and the chemical reduction of GO via bottom-up and top-down approaches [9].

Among the methods traditionally used to chemically prepare GO are the Brodie method, the Staudenmaier method, and Hummer's method, as well as the variations of the latter, namely the modified Hummer's method or the Improved Hummer's method [10]. The most frequently used chemical methods for preparing GO are listed in Table 1, along with their characteristics. The Brodie method, invented in 1859, was the first to synthesize graphite oxide by adding potassium chlorate ($KClO_3$) to a mixture of graphite and fuming nitric acid (HNO_3). Later, the Staudenmaier method was refined based on the Brodie method, with the addition of an intercalant composed of sulphuric acid (H_2SO_4) and HNO_3. This method resulted in the efficient production of graphite oxide. Both methods, however, required a lengthy oxidation step that could last up to four days. In 1958, the

Hummer method was widely adopted. It utilizes H_2SO_4 as an intercalant and sodium nitrate ($NaNO_3$)/potassium permanganate ($KMnO_4$) as an oxidant. Although this method involves a faster oxidation step, which is completed within two hours, it has been criticized for releasing toxic gases such as nitrogen dioxide (NO_2) and dinitrogen tetroxide (N_2O_4) into the environment. Recently, the Improved Hummer's method was developed by substituting $NaNO_3$ with a 1:9 mixture of H_2SO_4 and phosphoric acid (H_3PO_4). This method results in a more oxidized graphite oxide with a more regular carbon structure and a larger sheet size, while also avoiding the production of harmful gases [11].

Table 1. GO preparations made using chemical approaches.

Methods	Oxidants	Reaction Time (h)	Temperature (°C)	Advantages	Drawbacks	Ref.
Brodie method	$KClO_3$ HNO_3	72–96	60	• By using oxidation, laid the groundwork for graphite delamination into GO sheets	• Longer duration • Involves the threat of explosion • Tedious preparation	[12]
Staudenmaier method	HNO_3 H_2SO_4 $KClO_3$	96	90	• Enhances the yield	• Longer duration • Use of high temperature • Involves the threat of explosion	[13]
Hummer's method	$NaNO_3$ H_2SO_4 $KMnO_4$	~2	35,98	• Quicker • No danger of explosion • High effectiveness • High rate of return	• Production of toxic gases • Residual nitrates production	[14]
Improved Hummer's method	$KMnO_4$ H_3PO_4 H_2SO_4	12	50	• Temperature control is possible • Makes carbon substances that are hydrophilic • Faults are reduced • Free from the emission of harmful gases • High rate of return	• Longer duration • Requires twice as much $KMnO_4$ and 5.2 times as much H_2SO_4 as those used when applying Hummer's method	[15]

Apart from its ease of synthesis, the oxygenated groups in GO hold a number of advantages over graphene, including increased solubility and the ability to customize the surface functionalization for specific applications, resulting in a plethora of applications in nanocomposite materials [16]. Regardless of the advantages, the oxygen-containing functional groups must be removed to restore graphene's fundamental properties, most notably its electrical conductivity [17]. rGO is frequently referred to as a type of chemically synthesized graphene [18]. Numerous methods have been proposed for the preparation of rGO, including chemical, photo-mediated, thermal, and biological reduction [17,19]. The chemical reduction of exfoliated GO is the most frequently used method for producing rGO because it is cost-effective and rGO can be produced in large quantities [20]. In general, this procedure consists of two steps. The well-established method involves oxidizing graphite powder to form graphite oxide and then adding reducing agents to form rGO [21].

Numerous strong chemical reducing agents, including hydrazine [22], hydroquinone [23], dimethyl hydrazine, sodium borohydride ($NaBH_4$) [24], iron, tin powder [25], and zinc powder [26], have been used to synthesize rGO. However, the disadvantages of these

chemical reducing agents include their high toxicity; the presence of trace amounts of potentially harmful agents, particularly in bio-related applications such as catalysis and drug delivery [27]; and their environmental impact. Additionally, on an industrial scale, the costs of treating the toxic waste generated by the reduction reaction may rise significantly. As a result, numerous studies have predicted the use of green reductants in the development of a novel and environmentally friendly method for successfully converting GO to rGO under moderate conditions, in order to advance green technology. A green route is a simple, low-cost, non-toxic, and environmentally friendly procedure that utilizes materials and techniques that minimize the use and manufacture of hazardous compounds while avoiding the use of high temperatures and harsh reducing agents. Numerous phytochemicals derived from various plant parts, such as the peel, roots, seeds, leaves, and fruits, have been discovered to contain biomolecules. These biomolecules, which include proteins, polysaccharides, vitamins, pectins, amino acids, alkaloids, polyphenols, and flavonoids, may act as capping and reducing agents during the green reduction and formation of functional rGO from GO [28,29]. Phenolics and flavonoids are the most abundant type of secondary metabolites and bioactive molecules found in plants, and they are excellent antioxidants [30].

As a result, this study compiled a list of the previous and current green rGO synthesis methods that have outperformed traditional methods and may become the foundation of future sustainable material science research. Green synthesis is both cost-effective and environmentally friendly, releasing little or no pollution into the environment. The applications of generated rGO have been summarized to provide a brief overview. As listed in Table 2, numerous plant extracts were categorized by parts and are reported in order to aid in the reduction of GO.

Table 2. Summary of plant extracts utilized in the reduction of GO according to categories based on their parts.

No	Scientific Name	Reduction Method	Reduction Temperature (°C)	Reduction Time	Ref.
		Leaf Extract			
1	*Colocasia esculenta*	• stir • reflux	RT 100	8 h 5 h	[31]
2	*Mesua ferrea* L.	• stir • reflux	RT 100	10 h 8 h	
3	*Spinacia oleracea*	• stir	30	24 h	[32]
4	*Ginkgo biloba*	• stir	37	24 h	[33]
5	*Eichhornia crassipes*	• reflux	100	10 h	[34]
6	*Pulicaria glutinosa*	• reflux	98	24 h	[35]
7	*Prunus serrulate* *Magnolia Kobus* *Platanus orientalis* *Diopyros kaki* *Pinus desiflora* *Acer palmatum* *Ginkgo biloba*	• reflux	95	12 h	[36]
8	*Azadirachta indica*	• stir • reflux	RT 100	48 h 24 h	[37]
9	*Euphorbia wallichii*	• reflux	100	6 h	[38]
10	*Nicotiana tabacum* L.	• stir • reflux	RT 100	24 h 24 h	[39]

Table 2. *Cont.*

No	Scientific Name	Reduction Method	Reduction Temperature (°C)	Reduction Time	Ref.
11	*Spinacia oleracea*	• reflux	100	30 min	[40]
12	*Ficus religiosa* *Mangifera indica* *Polyalthia longifolia*	• reflux	50	24 h	[41]
13	*Artemisia vulgaris*	• reflux	90	6 h, 12 h	[42]
14	*Paederia foetide* L.	• stir	50	12 h	[9]
15	*Mangifera indica* L.	• stir • reflux	60 60–70	12 h 8 h	[43]
16	*Platanus orientalis*	• reflux	100	10 h	[44]
17	*Olea europaea*	• water bath	100	10 h	[45]
18	*Melissa officinalis* L.	• stir	RT	12 h	[46]
19	*Annona squamosa*	• reflux	100	12 h	[47]
20	*Eucalyptus*	• water bath	80	8 h	[48]
21	*Lantana camara*	• reflux	50	6 h	[28]
22	*Camellia sinensis*	• reflux	90	1 h	[49]
23	*Citrullus colocynthis*	• reflux	100	14 h	[50]
24	*Aloe vera*	• reflux	95	24 h	[51]
25	*Aloe vera* (L.) *Burm.f.*	• reflux	80	5 h	[52]
26	*Ocimum sanctum*	• reflux	100	10 h	[29]
27	*Anacardium occidentale Linn*	• stir	68	3 h	[53]
28	*Eucalyptus*	• reflux	80	8 h	[54]
29	*Ocimum sanctum* L.	• stir	70	4 h	[55]
30	*Stigmaphyllon ovatum*	• stir	60–70	24 h	[56]
31	*Euphorbia cheiradenia Boiss*	• reflux	80	7 h	[57]
32	*Mentha arvensis*	• reflux	80–95	3 h	[58]
33	*Tribulus terrestris* *Mentha piperita*	• autoclave	180	12 h	[59]
34	*Camellia sinensis*	• water bath	80	8 h	[60]
35	*Urtica dioica* L.	• stir	90	1 h	[61]
36	*Euphorbia milli*	• stir	RT	48 h	[62]
37	*Thymbra spicata*	• reflux	100	12 h	[63]
38	*Euphorbia heterophylla* (L.)	• reflux	95	12 h	[64]
39	*Memecylon edule*	• water bath	60	12 h	[65]
40	*Elaeis guineensis*	• reflux	100	3 h	[66]
41	*Zataria multiflora*	• reflux	98	24 h	[67]
42	*Memecylon edule*	• water bath	60	12 h	[65]
43 44	*Azadirachta indica* *Telfairia occidentalis*	• stir	30	24 h	[68]

Table 2. *Cont.*

No	Scientific Name	Reduction Method	Reduction Temperature (°C)	Reduction Time	Ref.
45	*Murraya koenigii*	• autoclave	100	12 h	[69]
46	*Cinnamomum camphora cineoliferum*	• stir	RT	24 h	[70]
47	*Phyllarthrom madagascariese* K. *Schum*				
48	*Acalypha indica*	• autoclave	100	12 h	[71]
49	*Erythrina senegalensis*	• reflux	95	24 h	[72]
50	*Callistemon viminalis*	• stir	60	2 h	[73]
		Fruit Extract			
1	*Cocos nucifera* L.	• oil bath	80, 100	12 h, 24 h, 36 h	[74]
2	*Punica granatum*	• stir	RT	12 h, 18 h, 24 h	[75]
3	*Vitis vinifera*	• reflux	95	1 h, 3 h, 6 h	[76]
4	*Terminalia bellirica*	• water bath	90	24 h	[77]
5	*Citrus limon*	• water bath	95	24 h	[78]
6	*Lycium barbarum*	• water bath	95	24 h	[79]
7	*Ficus carica*	• stir	95	12 h	[80]
8	*Zante currants*	• water bath	95	48 h	[81]
9	*Phyllanthus emblica*	• reflux	95	3 h	[82]
10	*Fragaria ananassa*	• reflux	95	12 h	[83]
11	*Phyllanthus emblica*	• autoclave	100	12 h	[84]
12	*Citrus grandis*	• reflux	95	12 h	[85]
13	*Tamarindus indica*				
14	*Terminalia bellirica*	• sonication	40	2 h	[86]
15	*Helicteres isora*				
16	*Quercus infectoria*				
		Flower Extract			
1	*Rosa damascena*	• autoclave	95	5 h	[87]
2	*Hibiscus sabdariffa* L.	• stir	100	1 h	[88]
3	*Syzygium aromaticum*	• reflux	100	30 min	[89]
4	*Chrysanthemum morifolium*	• water bath	95	24 h	[90]
5	*Tagetes erecta*	• stir	95	3 h	[91]
		Peel Extract			
1	*Citrus sinensis*	• stir	RT	10 h	[31]
		• reflux	100	8 h	
2	*Citrus limeta*	• reflux	50	6 h	[28]
3	*Sugarcane bagasse*	• stir	95	12 h	[92]
4	*Citrus hystrix*	• stir	RT	8 h	[93]

Table 2. *Cont.*

No	Scientific Name	Reduction Method	Reduction Temperature (°C)	Reduction Time	Ref.
		Bark/Stem Extract			
1	*Cinnamomum zeylanicum*	• reflux	100	45 min	[94]
2	*Cinnamomum verum*	• reflux	100	12 h	[95]
3	*Saccharum officinarum*	• stir • autoclave	50 150	3 h 12 h	[96]
4	*Cedrelopsis grevei Baill*	• stir	RT	24 h	[70]
5	*Alstonia scholaris*	• stir	90	1 h, 3 h	[97]
		Seed Extract			
1	*Phaseolus aureus* L.	• stir	30	24 h	[98]
2	*Terminalia chebula*	• reflux	90	24 h	[99]
3	*Glycine max* (L.) *Merr.*	• stir	75,85,95	1 h	[100]
4	*Vitis vinifera*	• stir	RT	10 h	[101]
5	*Punica grantum*	• stir	98	8 h	[102]
		Root Extract			
1	*Daucus carota*	• stir • reflux	RT 100	48 h 24 h	[103]
2	Asian red ginseng	• stirring in the presence of Fe foil as a catalyst	80	10 min	[104]
3	*Daucus carota subsp. sativus*	• stir	90	1 h	[105]
4	*Salvadora persica* L. *(miswak)*	• reflux	98	24 h	[106]
5	*Solanum tuberosum* L. *(potato)*	• stir • reflux	60 70–80	12 h 8 h	[43]
6	*Allium ascalonicum (shallot)*	• stir	RT	72 h	[107]
7	*Allium cepa (onion)*	• stir	RT	6 h	[108]
8	*Catharanthus roseus*	• precipitation	RT	24 h	[70]
9	*Raphanus sativus*	• autoclave	100	12 h	[71]
10	*Zingiber officinale Roscoe*	• reflux	90	4 h, 6 h, 8 h, 10 h,12 h	[109]
11	*Acorus calamus*	• sonication	40	2 h	[86]
		Pollen Grain Extract			
1	*Peltophorum pterocarpum*	• stir • heat-treated in an Ar gas • reflux • heat-treated in an Ar gas	RT 450 120 550	24 h 90 min 30 h 2 h	[110]

2. Preparation of Aqueous Extracts of Plants

The relevant portion of the plant was collected from local areas. The components were thoroughly cleaned to remove dust particles. Then the sample was either used fresh or dried in an air atmosphere, in the sun, or in an oven to remove the moisture. Following that, the dried components were ground into a fine powder using a mortar and pestle or a household blender. To prepare the extract, the powder or freshly chopped pieces were dispersed in distilled water and the solution was gradually heated using a magnetic stirrer, reflux, or Soxhlet apparatus. After allowing the mixture to cool to room temperature, it was filtered using filter paper to remove the bulk waste. The supernatant was collected and centrifuged to remove any detritus from the solution. The resulting filtrate was refrigerated and used to further reduce GO, as shown in Figure 1.

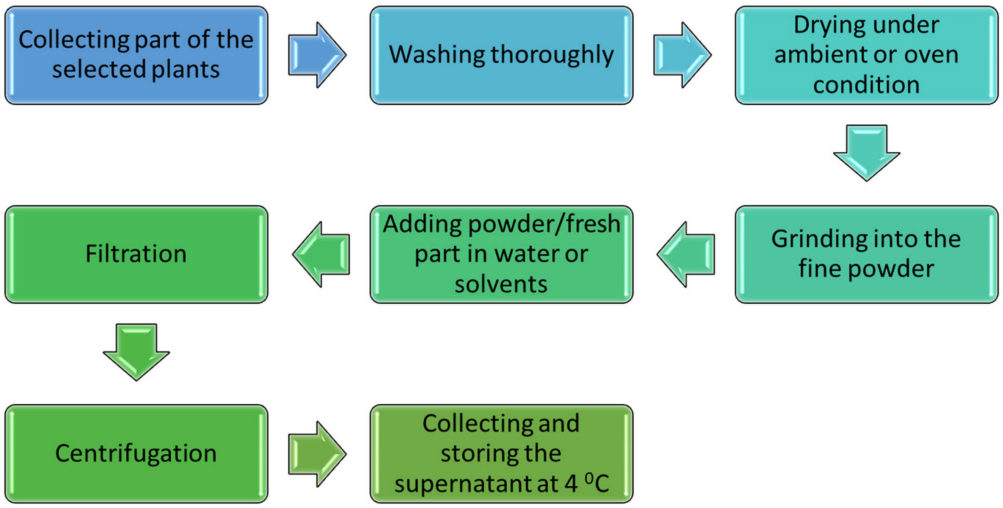

Figure 1. Preparation of plant aqueous extracts for the green synthesis of rGO using plant extracts.

3. The Synthesis of rGO

As illustrated in Figure 2, this synthesis procedure consisted of two steps. First, GO was prepared from graphite powder as a precursor. Second, deoxygenating agents were used to reduce the oxygen functional groups on the GO sheets. While organic solvents such as ethylene glycol, N,N-dimethyl formamide, and N-methyl pyrrolidine have been used to disperse GO, water is the most frequently used [111]. Sonication or magnetic stirring was performed to exfoliate the GO and create a homogeneous dispersion [22,112]. The resulting yellow-brown solution was used for reduction with the plant extracts. The mixture was then subjected to reflux, autoclave, or stirring at a controlled temperature of 24 °C to 180 °C for a duration of between 30 min to 72 h, based on previous studies. Adjusting the reaction solution pH with diluted sodium hydroxide (NaOH), hydrochloric acid (HCl), or ammonium hydroxide (NH_4OH) was also critical, as the reduction can occur in both acidic and alkaline environments [113]. Thus, based on a review of research on green reduction using plant extracts, the solution pH was primarily regulated using NH_4OH [44,45,50,61,65,76,77,80,81,95,99]. Bosch and colleagues demonstrated the effect of various pH values on the final production of GO sheets. Their results indicated that a reduction process conducted in an alkaline environment promotes the formation of minimal defects in the resulting rGO [114]. A change in the solution color from brownish to black indicated that the GO had been successfully deoxygenated. The solution was then filtered or centrifuged to obtain the black solid. The black solid was washed several times with water or alcohol to remove any impurities or plant residues. Finally, the collected black solid was allowed to dry at room temperature, in an oven, or in a vacuum freeze dryer. The resulting compound was designated as rGO.

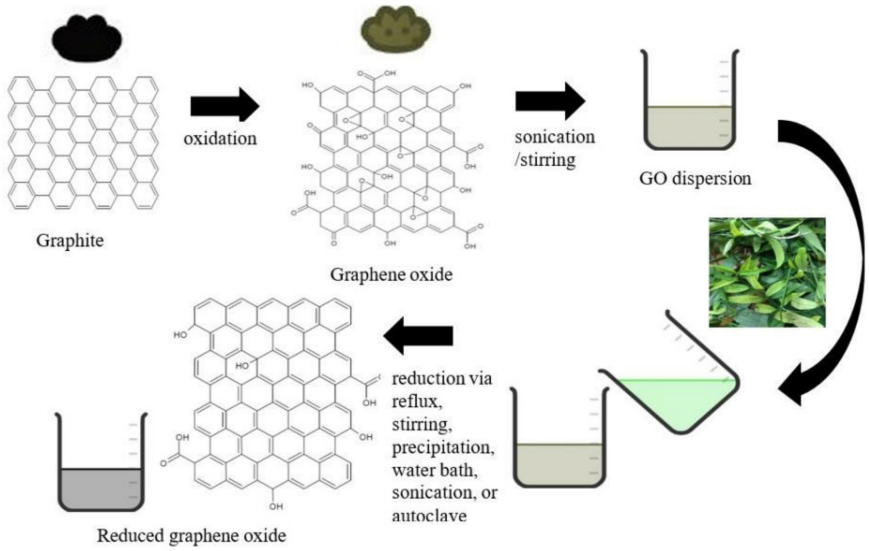

Figure 2. Schematic diagram of various steps involved in the synthesis of rGO.

4. Applications

The synthesis of rGO from natural and renewable resources is a vibrant and exciting area of research. As previously stated, eco-friendly routes have been developed by fusing green chemistry principles with nanotechnology to create biocompatible and bioactive nanodevices for a variety of applications, including photocatalysts, biomedical, sensors, and supercapacitors.

4.1. Biomedical Applications

Several reports in the literature describe the biomedical applications of green synthesis rGO. Gurunathan and co-workers demonstrated a successful reduction of GO using spinach leaf extract (S-rGO), which had significant biocompatibility with primary mouse embryonic fibroblast (PMEF) cells in various assays. These included cell viability, lactate dehydrogenase (LDH) leakage, and alkaline phosphate (ALP) activity [32]. Similarly, the research group synthesized graphene using *Ginkgo biloba* extract (Gb-rGO) and evaluated its biocompatibility with human breast cancer cells (MDA-MB-231) using a series of assays including cell viability, apoptosis, and ALP activity [33]. In terms of LDH leakage activity, the biocompatibility of S-rGO-treated PMEF cells showed no obvious differences, even at higher concentrations. The cytocompatibility of Gb-rGO-treated MDA-MB-231 cancer cells were determined using the TUNEL assay. Round and homogeneous nuclei cells were observed, with no TUNEL-positive cells. ALP is a membrane-bound enzyme involved in the mineralization of skeletal tissues; its activity has been used as a quantitative marker of osteoblastic differentiation [115]. It has been demonstrated that S-rGO-treated PMEF cells and Gb-rGO-treated MDA-MB-231 cancer cells enhanced ALP activity. S-rGO-treated PMEF cells and Gb-rGO-treated MDA-MB-231 cancer cells had no significant inhibitory effect on cell viability, even at the highest concentration (100 μg/mL).

The in vitro cytotoxicity of biosynthesized rGO using *Platanus orientalis* leaf extract against SICH cell line generated from the cardiac muscle of an Indian major carp (Catla catla) at various concentrations (3 μg/mL–72 μg/mL) [44]; rGO using *Erythrina senegalensis* leaf extract against SICH cell lines at various concentrations (10 μg/mL–100 μg/mL) [72]; and the synthesis of rGO using leaf extract of *Citrullus colocynthis* against human prostate cancer (DU 145) cell lines at various concentrations (4 mg/mL to 80 mg/mL) exhibited dose-dependent toxicity [50]. Shuba and colleagues demonstrated the synthesis of rGO using an *Ocimum sanctum* hydroalcoholic extract (ORGO). ORGO had lower hemolytic activity (by 4.3%) on suspended red blood cells from fresh chicken blood than GO at the highest concentration tested (10 μg/mL). The ORGO treatment of mouse embryonic fibroblast cells (Balb 3T3 cells) at various concentrations inhibited cell growth by 29% [29]. The cytotoxicity

of rGO loaded with paclitaxel synthesis from *Euphorbia milli* leaves against human lung cancer cell lines (A549) decreased with increasing concentrations (0 to 500 µg/mL). The free rGO exhibited negligible cytotoxicity toward A549 cell lines [62]. The in vitro cytotoxicity of rGO nanosheets derived from *Euphorbia heterophylla* (L.) leaf extracts against cancerous cell lines, such as Human Hepatocarcinoma (HepG2) and A549 cell lines, was found to decrease with increasing concentrations (0 to 400 µg/mL). The mechanism of the action of rGO against cancer cell lines is unknown. The rGO may interact with the plasma membrane or extracellular matrix, entering the cell primarily via diffusion, endocytosis, and/or binding to receptors [64].

Wang et al. [65] demonstrated the synthesis of rGO from *Memecylon edule* leaf extracts, which could potentially be used as a photothermal therapeutic agent for cancer cell apoptosis. Even at the highest concentration (1 mg/mL), the biocompatibility of synthesized rGO was independent of the concentration and resulted in cell viability of >98% in the Madin-Darby Canine Kidney (MDCK) and A549 cell lines examined. However, when cells were exposed to near-infrared light, rGO-treated A549 cells demonstrated a rapid decline in viability (from 65% to 35%), whereas rGO-treated MDCK cells demonstrated a slow decline in viability (from 90% to 65%). Thus, upon NIR irradiation, the PTT agents emitted the greatest amount of photothermal heat within the tumor atmosphere, resulting in the greatest photothermal cytotoxicity in the A549 cells. In comparison, the PTT agents exhibited the least photothermal cytotoxicity on typical MDCK cells due to the absence of a responsive atmosphere.

Punniyakotti et al. [71] investigated the deoxygenation of GO using two distinct types of green extracts, *Acalypha indica* (AIrGO) and *Raphanus sativus* (RSrGO), and their anticancer activity against human breast (MCF-7) and A549 cancer cell lines. Cell inhibition was 61.34% (IC_{50} 38.46 µg/mL) for the AIrGO-treated A549 cells and 65.84% (IC_{50} 26.69 µg/mL) for the RSrGO-treated A549 cells at the maximum concentration (100 µg/mL). At a concentration of 100 µg/mL, AIrGO inhibited MCF-7 cells by 68.55% (IC_{50} 35.97 µg/mL) and RSrGO inhibited MCF-7 cells by 71.15% (IC_{50} 33.22 µg/mL). *Acorus calamus* (ACCARGO), *Terminalia bellirica* (TBRGO), *Helicteres isora* (HIRGO), and *Quercus infectoria* (QIRGO) rGO-mediated herbal plant extracts exhibited significant concentration-dependent cytotoxicity against MCF-7 cell lines [86]. ACARGO inhibited cell growth by 20.2% (IC_{50} 81 µg/mL), TBRGO by 26% (IC_{50} 120 µg/mL), HIRGO by 30% (IC_{50} 92 µg/mL), and QIRGO by 31.1% (IC_{50} 87 µg/mL).

The anti-tuberculosis activity of rGO synthesized from bark extracts of *Cinnamomum verum* was demonstrated against *Mycobacterium tuberculosis* H37Ra (*M. tuberculosis* H37Ra) [95]. The MABA assay demonstrated that rGO-treated *M. tuberculosis* H37Ra exhibited anti-tuberculosis activity at 200 µg/mL. Yaragalla et al. [101] demonstrated the deoxygenation of GO using grape seed extract and evaluated its antimicrobial and anti-proliferation activity. The antibacterial activity of rGO against *Staphylococcus aureus* (*S. aureus*) and *Escherichia coli* (*E. coli*) at various concentrations revealed that bacteria were completely killed at the higher concentrations (4 and 5 µg/mL). Heat-induced inflammatory activity, measured by aspirin (the standard drug) and rGO on RBC suspension, revealed no statistically significant differences, with rGO demonstrating 39.83% activity and aspirin demonstrating 41.34% activity. The in vitro anti-proliferation activity of rGO on human colon carcinoma (HCT-116) cell lines was found to be approximately 88% effective at the highest concentration (500 µg/mL) within 24 h.

In 2019, Khanam and Hasan synthesized graphene from *Allium cepa* (onion) extracts and evaluated its antibacterial properties against two gram-negative bacteria (*E. coli* and *Pseudomonas aeruginosa*) as well as two gram-positive bacteria (*Streptococcus faecalis* and *S. aureus*). The percentage loss of cell viability on the fifth day (120 h) was 90.5% for *E. coli* treated with rGO, 93.1% for *P. aeruginosa* treated with rGO, 94% for *S. faecalis* treated with rGO, and 95% for *S. aureus* treated rGO. The results indicated that antibacterial activity was more effective against gram-positive bacterial cells [108]. In 2013, Akhavan and colleagues demonstrated that rGO mediated by Asian red ginseng promoted human neural stem

cell (hNSC) attachment and proliferation due to the presence of ginsenosides (a potent antioxidant) on the rGO sheet surface. Additionally, using immunofluorescence imaging as an evaluation tool, ginseng-rGO films were shown to exhibit greater differentiation of hNSCs into neurons rather than glial cells [104]. Table 3 below lists the biomedical applications of green rGO using various plant extracts, as well as their bioactivity (cytotoxicity, anti-microbial, anti-tuberculosis, and anti-proliferative).

Table 3. Summary of the biocompatibility of rGO synthesis using cytotoxicity, anti-microbial, anti-tuberculosis, and anti-proliferative properties.

Scientific Name	Activity	Cell Lines	Strain	MIC	Concentration	Cell Viability (%)	IC_{50}	Ref.
Spinacia oleracea	Cytotoxicity	• Primary mouse embryonic fibroblast (PMEF)	NA	NA	• 10–100 µg/mL	• 100	NA	[32]
Citrullus colocynthis	Cytotoxicity	• Prostate cancer (DU 145)	NA	NA	• 4 mg/mL • 8 mg/mL • 40 mg/mL • 80 mg/mL	• 86 • 70 • 36 • 20	NA	[50]
Ocimum sanctum	Cytotoxicity	• Mouse fibroblast (Balb 3T3)	NA	NA	• 10 µL	• 29	NA	[29]
Euphorbia milli	Anticancer effect of rGO loaded paclitaxel	• Lung cancer (A549)	NA	NA	• 200 µg/mL • 500 µg/mL	• 29 • 10	NA	[62]
Euphorbia heterophylla (L.)	Cytotoxicity	• Lung cancer (A549) • Hepatocarcinoma (HepG2)	NA NA	NA NA	• 25 µg/mL • 50 µg/mL • 100 µg/mL • 200 µg/mL • 400 µg/mL • 25 µg/mL • 50 µg/mL • 100 µg/mL • 200 µg/mL • 400 µg/mL	• 89.76 • 66.29 • 64.05 • 54.25 • 43.85 • 99.79 • 88.03 • 81.44 • 64.50 • 47.66	• 297.81 µg/mL • 357.53 µg/mL	[64]
Memecylon edule	Cytotoxicity	• Lung cancer (A549) • Madin-Darby Canine Kidney (MDCK) • A549 with near-infrared light irradiation • MDCK with near-infrared light irradiation	NA	NA	• 1 mg/mL • 1 mg/mL • 0.001 mg/mL to 1 mg/mL • 0.001 mg/mL to 1 mg/mL	• >98 • >98 • 65 to 35 • 90 to 65	NA	[65]
Acalypha indica	Cytotoxicity	• Breast cancer (MCF-7) • Lung cancer (A549)	NA	NA	• 100 µg/mL • 100 µg/mL	• 68.55 • 61.34	• 35.97 µg/mL • 38.46 µg/mL	[71]
Raphanus sativus	Cytotoxicity	• Breast cancer (MCF-7) • Lung cancer (A549)			• 100 µg/mL • 100 µg/mL	• 71.15 • 65.84	• 33.22 µg/mL • 26.69 µg/mL	

Table 3. *Cont.*

Scientific Name	Activity	Cell Lines	Strain	MIC	Concentration	Cell Viability (%)	IC_{50}	Ref.
Acorus calamus	Cytotoxicity	• Breast cancer (MCF-7)	NA	NA	• 50 µg/mL • 100 µg/mL • 150 µg/mL • 200 µg/mL • 250 µg/mL	• 97.2 • 53.3 • 35.1 • 23.1 • 20.2	• 81 µg/mL	[86]
Terminalia bellirica					• 50 µg/mL • 100 µg/mL • 150 µg/mL • 200 µg/mL • 250 µg/mL	• 97 • 76 • 45 • 32 • 26	• 120 µg/mL	
Helicteres isora					• 50 µg/mL • 100 µg/mL • 150 µg/mL • 200 µg/mL • 250 µg/mL	• 98.1 • 57.4 • 35.3 • 27.2 • 30	• 92 µg/mL	
Quercus infectoria					• 50 µg/mL • 100 µg/mL • 150 µg/mL • 200 µg/mL • 250 µg/mL	• 96 • 54.4 • 36.2 • 29.3 • 31.1	• 87 µg/mL	
Allium cepa	Anti-bacterial	NA	• *Streptococcus faecalis* • *Staphylococcus aureus* • *E. coli* • *Pseudomonas aeruginosa*	NA	• 10 µg/mL	• 24 h: 52 • 120 h: 94 • 24 h: 54 • 120 h: 95 • 24 h: 45 • 120 h: 90.5 • 24 h: 49 • 120 h: 93.1	NA	[108]

4.2. Supercapacitors

Several reports in the literature describe the supercapacitor applications of green synthesized rGO. Chu and colleagues (2014) demonstrated how synthesized rGO from an aqueous extract of *Hibiscus sabdariffa* L. (HRGO) was used to fabricate a flexible graphene film electrode. The electrical conductivity of the HRGO electrodes significantly increased, by over four orders of magnitude, by treating them in a household microwave oven (MW-HRGO-R). The electrode's specific capacitance increased as the scan rate decreased for both the HRGO-R and MW-HRGO-R cells [88]. The green reduction of GO and the fabrication of an open porous structure were accomplished simultaneously in a one-pot process utilizing an aqueous seed extract of *Glycine Max* (L.) *Merr.* and the presence of protein gelation, designated as BRGO and BRGO-H, respectively. BRGO-H exhibited excellent electrical conductivity, a high swelling ratio, and an open porous structure, while graphene coated with soybean proteins was used as a starting material for the fabrication of graphene-based porous electrodes. To further improve the electrode's electrical conductivity and efficiency, BRGO-H was microwave-treated to form a graphene-based nanocomposite. Thus, electrical conductivity was increased by approximately four orders of magnitude and the electroactive surface area was increased more than fourfold. The increased specific capacitance indicated a promising application for supercapacitor electrodes [100].

Jana and coworkers (2014) demonstrated that rGO synthesized from mung beans (*Phaseolus aureus* L.) soaked in water had a high specific capacitance and excellent electrochemical cyclic stability, making it an excellent candidate as a supercapacitor electrode material [98]. Another study by a similar group demonstrated that rGO synthesized from a tobacco solution at a temperature of 100 °C outperformed rGO synthesized at room temperature as a supercapacitor electrode material [39]. Green synthesis of rGO prepared from *Peltophorum pterocarpum* pollen grains demonstrated excellent electrochemical properties with a maximum specific capacitance of 27.1 F g^{-1}, which could potentially be used to fabricate bilayer capacitors [110]. The electrochemical properties of *Aloe vera* (L.) *Burm. f.* extract containing rGO revealed a specific capacitance of 142 F g^{-1} (at a scan rate of 5 mV s^{-1}), a galvanostatic charge-discharge capacitance of 267 F g^{-1} (at a current density

1 A g^{-1}), and a cyclic stability capacitance of 158 F g^{-1} for 1000 cycles. The electrochemical results for the rGO demonstrated its high potential for use in developing electrodes for supercapacitor-based energy storage devices [52].

Raja et al. (2019) demonstrated the electrochemical performance of rGO using strawberry extract. They discovered that as the scan rate decreased, the specific capacitance increased from 39.4 F g^{-1} at a scan rate of 50 mV s^{-1} to 230.4 F g^{-1} at a scan rate of 10 mV s^{-1}. Additionally, the rGO retained 81% of its specific capacitance after 500 cycles [89]. The deoxygenation of GO using *Citrus grandis* and *Tamarindus indica* revealed excellent conductivity (47.33 F g^{-1} and 65.25 F g^{-1}, respectively) and high specific capacitance (4090 Sm^{-1} and 5545 Sm^{-1}, respectively), making them suitable materials for supercapacitor applications [85]. The rGO that employed aqueous ginger extract refluxed at 90 °C for 12 h demonstrated excellent electrical conductivity, the highest specific capacitance value, and charge-discharge cyclic stability. The rGO material showed it could potentially be mass-produced and used as an electrode material for supercapacitors [109]. Table 4 shows a summary of the electrochemical performance of various samples of synthesized rGO.

Table 4. Summary of the electrochemical performance of synthesized rGO samples.

Scientific Name	Resistance	Specific Capacitance	Charge-Discharge Cyclic Stability	Ref.
Hibiscus sabdariffa L.	• Before microwave • 0.63 MΩ/sq sheet resistance • After microwave • 36.50 MΩ/sq sheet resistance	• 133.07 F g^{-1} at 5 mVs^{-1} • 204.38 F g^{-1} at 5 mVs^{-1}	NA	[88]
Phaseolus aureus L.	• 10 Ω solution resistance	• 137 F g^{-1} at 1.3 A g^{-1}	98% after 1000 cycles	[98]
Nicotiana tabacum	• 4.20 Ω solution resistance	• 206 F g^{-1} at 0.16 A g^{-1}	~112% after 1000 cycles	[39]
Peltophorum pterocarpum	NA	• 27.1 F g^{-1} at 5 mVs^{-1}	NA	[110]
Black soybean	• Before microwave • 15 MΩ/sq sheet resistance • After microwave • 1.5 kΩ/sq sheet resistance	• 27 F g^{-1} at 1 mVs^{-1} • 180.4 F g^{-1} at 1 mVs^{-1}	90% after 1000 cycles	[100]
Aloe vera (L.) *Burm. f.* mediated rGO	NA	• 142 F g^{-1} at 5 mVs^{-1}	NA	[52]
Fragaria ananassa	NA	• 230.4 F g^{-1} at 10 mVs^{-1} • 236 F g^{-1} at 1 A g^{-1}	81% at 500 cycles	[83]
Citrus grandis	• 4090 Sm^{-1} sheet resistance	• 65.25 F g^{-1} 25 mVs^{-1}	NA	[85]
Tamarindus indica	• 5545 Sm^{-1} sheet resistance	• 47.33 F g^{-1} at 25 mVs^{-1}		
Ginger	• 14.6 Ω	• 99.61 F g^{-1} 5 mVs^{-1}	98% after 1000 cycles	[109]

4.3. Photocatalytic Degradation

Several reports in the literature describe the degradation applications of green synthesized rGO. Singh and colleagues (2018) synthesized rGO sheets (rG1-sugar cane juice and hydrazine hydrate) and a disc structure, using sugarcane juice as a reducing agent (rG2-sugarcane juice). The photocatalytic degradation of phenanthrene (PHE) using the synthesized rGO was further investigated under UV irradiation. PHE is one of the most prevalent polycyclic aromatic hydrocarbons (PAHs) in the environment, being produced continuously by various sources. PAHs pose a serious threat to the environment and human health due to their hazardous and carcinogenic nature. Pure PHE degrades at a rate of 5%, whereas rG1 and rG2 degrade at rates of 25% and 30%, respectively. Due to the spherical disc-like structures, rG2 degrades PHE more efficiently than rG1. In comparison to the sheet structure, it contains a greater number of active catalytic sites for interaction with the PHE molecules [96].

Mahata et al. [55] demonstrated that rGO synthesized from *Ocimum sanctum* L. leaf extract is an efficient catalyst when used in combination with $NaBH_4$ in water for the regioselective reduction of α, β-unsaturated carbonyl compounds to their allylic alcohols. When the catalyst loading was increased from 10 mg to 15 mg, the yield of the products increased by up to 92%. However, increasing the catalyst concentration did not result in a higher conversion rate, indicating that 15 mg is the optimum catalyst loading. Another study conducted by the same group demonstrated that GO could be reduced using *Anacardium occidentale Linn* (Cashew) leaf extract (CLRG) as a bio-renewable catalyst. The catalytic activity of CLRG was demonstrated to successfully reduce nitrobenzene to aniline with a yield of 94% in four hours. As a result, the prepared rGO efficiently catalyzed the electro-/chemical transformation of nitro to an amine group [53]. Suresh et al. demonstrated that rGO derived from *Spinacia oleracea* (leaf extract), *Syzygium aromaticum* (bud extract), and *Cinnamomum zeylanicum* (bark extract) completely degraded carcinogenic dye methylene blue (MB) and malachite green (MG) in the presence of 20 mg rGO [40,89,94].

Jin and co-workers (2018) reported the adsorptive capacity of biosynthesized rGO containing *Eucalyptus* leaf extract compared to that of other adsorbents, including activated carbon, graphite powder, and commercial graphene. The maximum adsorption capacity of various adsorbents was determined to be rGO> commercial graphene> activated carbon> graphite powder. The rGO's high dispersibility means it adheres to the surface of biomolecules and increases the contact surface area with the MB [54]. As a green reducing agent, rGO prepared from Aloe vera demonstrated a remarkable capacity for dye removal, with a maximum efficiency of 98% achieved. The strong electrostatic interaction between the MB and rGO molecules, the strong π–π interaction between the MB molecules, and the increased surface area of the rGO all contributed to the increased adsorption efficiency. The recyclability of the synthesized rGO for up to five adsorption cycles with no significant loss of capability makes it an attractive candidate as an industrial dye adsorbent material [51].

The adsorption capacity (q_{max}) of rGO synthesized from *Citrus hystrix* peel extract on MB was determined to be 276.06 mg/g at room temperature [93]. Ghosh et al. [97] reported the photocatalytic activity of rGO synthesis using the bark extract of *Alstonia scholaris* (with a duration of three hours) toward MB and methyl orange (MO). It has been demonstrated that MB degrades at a rate of 95.29%, whereas MO degrades at a rate of only 6%. As a result, the rGO would be significantly more effective at removing cationic dye from wastewater than it would at removing anionic dye.

Parthipan et al. [69,84] investigated the photocatalytic activity of rGO biosynthesized from *Phyllanthus emblica* fruit extracts (PErGO) and *Murraya koenigii* leaf extract (MKrGO) against MB, MO, and mixed (MB + MO) dye solutions when exposed to sunlight and UV light. PErGO treated with a mixed dye solution (MB + MO) and exposed to sunlight demonstrated degradation efficiencies of 9% and 91% for the MO and MB dyes, respectively. Within 120 min of exposure to natural sunlight, the catalyst MKrGO was shown to degrade approximately 80% and 77% of the MO and MB dyes, respectively. This implies that sunlight exposure is the best option for both dye molecules in the presence of the catalyst

rGO. This catalyst's stability was maintained with only minor changes over the course of five degradation cycles.

Sugarcane bagasse extract was used to remove cadmium (Cd (II)), with an adsorption capacity of nearly 24.47 mg/g. This demonstrated rGO's potential for removing heavy metals from wastewater [92]. Moosa and Jaafar (2017) demonstrated that rGO mediated by *Camellia sinensis* (black tea) leaf extract added to sand showed a high level of removal efficiency for lead ions in an aqueous solution. As the concentration of lead ions increased, the removal efficiency decreased due to the lead ion saturation of the adsorption sites [49]. Lin et al. [60] demonstrated rGO prepared from green tea extract (*Camellia sinensis*) successfully removed Pb (II) from an aqueous solution under various experimental conditions that included pH, temperature, adsorbent dose, and adsorbate concentration. The excellent removal efficiency of Pb (II) was determined to be 96.6% under the operating conditions of 10 mg/L Pb (II) and 0.4 g/L rGO with a pH of 4.5 at 30 °C. The rGO was recyclable up to four times at the cost of only a partial adsorption capacity (first cycle—97.4%, second cycle—96.7%, third cycle—87.8%, and fourth cycle—80.0%) [60].

It was demonstrated that the biological synthesis of rGO from *Callistemon viminalis* leaf extract could p be used as a membrane filter for the removal of heavy metal ions from drinking water. The highest iron rejection rate of 95.77% was obtained when a greater amount of rGO (0.10 g) nanomaterial was used in the membrane. This rGO was used to remove heavy metals using a low-pressure driving force, and the increased hydrophilicity of the membrane resulted in a smoother water flux over a longer period [73].

Table 5 summarizes various catalytic studies utilizing rGO prepared using various plant extracts, together with the concentration used, degradation time, percentage of removal, and adsorption capacity.

Table 5. Summary of the catalytic activity of synthesized rGO.

Scientific Name	Dye Used	Metal Ions	Concentration	Amount of Photo-Catalyst	Time Required for Degradation (min)	Feature	% Removal	Adsorption Capacity	Ref.
Spinacia oleracea	Methylene blue (MB) Malachite green (MG)	NA	• 100 mL of 5 ppm solution	• 20 mg	• 60 min • 40 min	• Dark condition	NA	NA	[40]
Syzygium aromaticum	Methylene blue (MB) Malachite green (MG)	NA	• 100 mL of 5 ppm solution	• 20 mg	• 20 min	• Dark condition	NA	NA	[89]
Cinnamomum zeylanicum	Methylene blue (MB) Malachite green (MG)	NA	• 100 mL of 5 ppm solution	• 20 mg	• 40 min	• Dark condition	NA	NA	[94]
Eucalyptus	Methylene blue (MB)	NA	• 20 mL of 50 mg L^{-1}	• 0.02 g	• 10	NA	NA	~45 mg/g	[54]
Camellia sinensis	NA	Lead	• 155.5 ppm • 240.5 ppm • 299 ppm	NA	NA	NA	• 99.9% • 99.9% • 92%		[49]
Sugarcane bagasse	NA	Cadmium	• 25 mL of Cd (II) (20 mg/L)	• 12 mg	NA	NA	NA	24.47 mg/g	[92]
Aloe vera	Methylene blue (MB)	NA	• 125 mL in 4 ppm solution	• 20 mg	NA	NA	• 98%	NA	[51]
Camellia sinensis	NA	Lead (Pb (II))	• 150 mL of 10 mg/L solution	• 0.4 g/L	NA	NA	• 96.6%		[60]
Citrus hystrix	Methylene blue	NA	• 20 mL of 50 mg/L	• 5 mg	NA	NA	NA	276.06	[93]
Callistemon viminalis	NA	Iron	NA	NA	NA	NA	• 95.77%	NA	[73]

Table 5. *Cont.*

Scientific Name	Dye Used	Metal Ions	Concentration	Amount of Photo-Catalyst	Time Required for Degradation (min)	Feature	% Removal	Adsorption Capacity	Ref.
Alstonia scholaris	Methylene blue (MB) Methyl orange (MO)	NA	• 50 mL of 12 mg L^{-1}	• 10 mg	NA	NA	• 95.29% • 6.03%	NA	[97]
Phyllanthus emblica	Mixed dye (MB + MO) Mixed dye (MB + MO)	NA	• 10 mg/L	• 20 mg/L	• 90 min	• Sunlight exposure • UV	• 91% (MB) • 92% (MO) • 98% (MB) • 49% (MO)	NA	[84]
Murraya koenigii	Methylene blue Methyl orange	NA	• 10 mg/L	• 20 mg/L	• 120 min	• Sunlight exposure	• 77% • 80%	NA	[69]

4.4. Antioxidant

Suresh and co-workers demonstrated that rGO mediated with *Spinacia oleracea* (leaf extract), *Syzygium aromaticum* (bud extract), and *Cinnamomum zeylanicum* (bark extract) showed scavenging activity against DPPH free radicals with IC_{50} values of 1590 µg/mL, 1337 µg/mL, 2250 µg/mL, respectively [40,89,94].

4.5. Sensors

In 2013, Haghighi and Tabrizi demonstrated the use of *Rosa damascene* (rose water) as a reducing agent for GO reduction, while its capacity to fabricate new types of sensors and biosensors was investigated using electrochemical measurements. Electrochemical impedance spectroscopy (EIS) measurements revealed that the rGO-modified glassy carbon electrode (GCE) had a charge transfer resistance (R_{ct}) of 180 Ω and a peak-to-peak separation of 96 mV for the redox probe. By examining the electrochemical properties of catechol in a phosphate buffer solution and nicotinamide adenine dinucleotide (NADH) using a modified GCE/rGO electrode, the applicability of the prepared rGO for the fabrication of a new type of modified electrode was determined. The GCE/rGO redox peaks for catechol had a formal potential of 140 mV vs. Ag/AgCl and a peak-to-peak separation of 97 mV, whereas NADH oxidation had a formal potential of 340 mV vs. Ag/AgCl. Further studies on modified GCE/rGO electrodes with immobilized glucose oxidase (GO_x) revealed redox peaks with a formal potential of −412 mV vs. Ag/AgCl and a 45 mV peak-to-peak separation. The results demonstrated that the synthesized rGO accelerated the electron transfer rate of a redox probe across the modified electrode interface. The electrocatalytic activity of GCE modified with rGO was excellent for catechol, NADH, and immobilized GO_x [87].

A few years later, Chettri and colleagues demonstrated that 3D hedgehog-like nanostructures could self-assemble on the rGO surface without the use of external precursors. This enabled the rGO to be used effectively as a template for the development of high-performance energy storage and biosensing devices [42]. The researchers used rGO mediated with olive leaves to create a conductive indium tin oxide (ITO)/rGO-modified electrode. Cyclic voltammetry was used to investigate the electrochemical properties of the ITO/rGO electrode and to demonstrate the response in both the presence and absence of ascorbic acid. The ITO/rGO electrode had a larger cyclic voltammetry area (quasi-rectangular shape) and a higher specific capacitance (275 F g^{-1}), indicating that it was a successful ascorbic acid sensor. As a result, this rGO was deemed suitable for use as an electrode modifier in energy storage devices and as an AA sensor [45]. Ghosh and colleagues demonstrated how to reduce GO to green rGO (GRGO) using different green reagents, including starch, ascorbic acid, glucose, clove extract, and mint extract. All the GRGO samples were found to have slightly higher electrical conductivities. Cyclic voltam-

metry and impedance measurements on all the GRGO samples indicated that the GRGO mediated with the mint leaf extract modified electrode had the highest current-voltage response, as well as the lowest charge transfer resistance of 140 Ω (R_{ct}) [58].

4.6. Nanocomposite

Atarod et al. (2015) synthesized nanocomposite by the biological reduction of GO, copper, and iron oxide (Cu/RGO/ Fe_3O_4) using *Euphorbia wallichii* leaf extract as a magnetically recoverable catalyst for the reduction of 4-nitrophenol (4-NP) to 4-aminophenol (4-AP) in the presence of $NaBH_4$ and Rhodamine B (RhB) dye in water at room temperature. The Cu/RGO/Fe_3O_4 nanocomposite was found to be highly active and could be recycled with no significant loss of activity for approximately six catalytic cycles [38]. rGO was synthesis from *Melissa officinalis* extract and combined with hydroxyapatite (HA) in various concentrations to form rGO-HA nanocomposite. The rGO-HA (1%) composite was determined to be the optimal composition, with a 3.2-fold increase in strength compared to pure HA. The biocompatibility of rGO-HA nanocomposite at 1% and 0.5% concentrations was evaluated using NIH-3T3 fibroblast cells [46].

Elmike and colleagues in 2019, demonstrated the fabrication of rGO, zinc oxide nanoparticles (ZnO), silver-zinc oxide nanoparticles (AgZnO), and rGOAgZnO nanocomposite using *Stigmaphyllon ovatum* leaf extract. Over 120 min of photocatalytic degradation of MB using the nanomaterials, the nanocomposite demonstrated the highest degradation efficiency of 68.1, 62.7, 61.7, and 57.4% for the rGOAgZnO, ZnO, rGO, and AgZnO respectively [56]. Copper nanoparticles (Cu NPs) were deposited on rGO using *Euphorbia cheiradenia* leaf extract to form the Cu/rGO nanocomposite, which demonstrated excellent degradation of 4-nitrophenol and hazardous dyes such as rhodamine B, methylene blue, methyl orange, and congo red using $NaBH_4$ at room temperature. Cu/rGO nanocomposite has a five-cycle reusability potential without deteriorating its catalytic capability [57].

A bioinspired approach was used to synthesize a palladium-anchored *Thymbra spicata* extract-modified graphene oxide nanohybrid material (Pd NPs/rGO-*T. spicata*). The nanohybrid material demonstrated excellent water dispersibility. The as-prepared material was demonstrated to be a heterogeneous catalyst for cyanating aryl halides (X = I, Br, Cl) using potassium hexacyanoferrate (II) trihydrate as a relatively inexpensive source of cyanide. The catalysts could be recovered and reused up to eight times without significantly reducing their catalytic activity [63]. Khojasteh and colleagues investigated the reduction of GO to rGO using leaf extracts of *Metha piperita* and *Tribulus terrestris*, which both demonstrated moderate antioxidant activity in the DPPH assay (IC_{50} = 28 and 33 ppm, respectively). The *Mentha piperita* extracts reduced GO more effectively than the *Tribulus terrestris* extracts. Additional studies on the reducibility of *Mentha piperita* extract were conducted using the synthesized rGO/Fe_3O_4 nanocomposite. Vibrating sample magnetometer analysis indicated that the appropriate reduction of Fe ions and GO resulted in the formation of an rGO/Fe_3O_4 nanocomposite with superparamagnetic properties [59].

5. Characterizations

The reduction of GO to rGO with green reductants can be characterized using various optical, structural, electrochemical, and thermal techniques to confirm the removal of oxygen moieties, as listed in Figure 3. The optical properties were investigated using ultraviolet-visible spectroscopy (UV-Vis), whereas the development of the crystalline structure was studied using X-ray diffraction (XRD). The functional groups were identified using Fourier transform infrared spectroscopy (FTIR) and the electronic structures were deduced using Raman spectroscopy. The atomic composition and chemical covalent bond details were determined using X-ray photoelectron spectroscopy (XPS). The sheet thickness was determined using atomic force microscopy (AFM). To observe the morphology and examine the microstructures, field emission scanning electron microscopy (FESEM) and transmission electron microscopy (TEM) were used. The thermal stability and thermal degradation properties were determined using thermogravimetric analysis (TGA) and

differential scanning calorimetry (DSC). The average size and potential surface charge were determined using dynamic light scattering (DLS). Cyclic voltammetry was used to determine the electroactive surface area, while four-point probe resistivity was used to determine the sheet resistance.

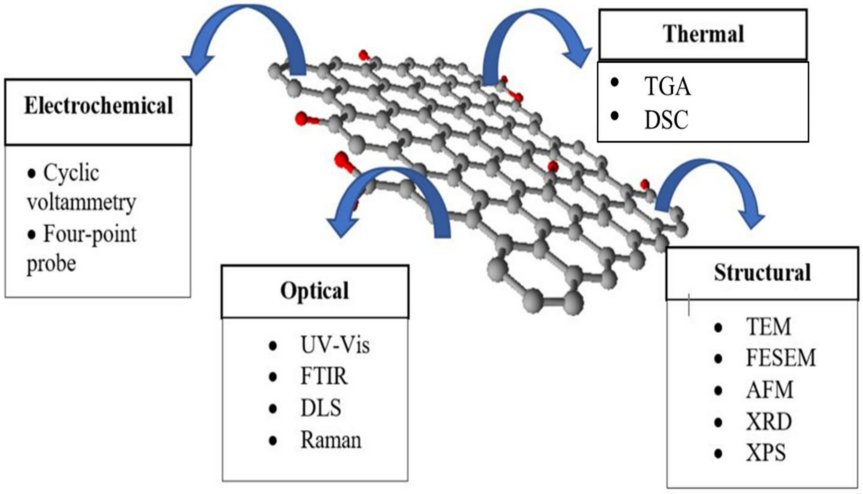

Figure 3. Characterization techniques used to verify the properties of successful rGO synthesis.

6. Conclusions

To summarize, nature contains a vast number of plant species, many of which have considerable potential for further exploration and investigation in order to produce green nanomaterials. The majority of plant parts, such as the leaves, roots, bark, stems, fruits, and seeds, are now being used to synthesize GO and rGO. This has proven to be a more sustainable, reliable, and feasible method than the chemical method. The major advantages of using green reductants are that they are environmentally friendly, cost-effective, non-toxic, biocompatible, and readily available. It is also simple to isolate the product. In summary, rGO prepared by utilizing the green route can potentially be extremely useful in a wide variety of applications and in opening new avenues for bulk production.

Author Contributions: Conceptualization, C.A.C.A., D.P. and E.L.A.; writing—original draft preparation, D.P.; writing—review and editing, C.A.C.A., D.P. and E.L.A.; visualization, D.P.; supervision, C.A.C.A. All authors have read and agreed to the published version of the manuscript.

Funding: This research received no external funding.

Conflicts of Interest: The authors declare no conflict of interest.

References

1. Paton, K.R.; Varrla, E.; Backes, C.; Smith, R.J.; Khan, U.; O'Neill, A.; Boland, C.; Lotya, M.; Istrate, O.M.; King, P.; et al. Scalable production of large quantities of defect-free few-layer graphene by shear exfoliation in liquids. *Nat. Mater.* **2014**, *13*, 624–630. [CrossRef] [PubMed]
2. Novoselov, K.S.; Geim, A.K.; Morozov, S.V.; Jiang, D.; Zhang, Y.; Dubonos, S.V.; Grigorieva, I.V.; Firsov, A.A. Electric field in atomically thin carbon films. *Science* **2004**, *306*, 666–669. [CrossRef] [PubMed]
3. Liu, Y.; Yu, D.; Zeng, C.; Miao, Z.; Dai, L. Biocompatible graphene oxide-based glucose biosensors. *Langmuir* **2010**, *26*, 6158–6160. [CrossRef] [PubMed]
4. Sun, X.; Liu, Z.; Welsher, K.; Robinson, J.T.; Goodwin, A.; Zaric, S.; Dai, H. Nano-graphene oxide for cellular imaging and drug delivery. *Nano Res.* **2008**, *1*, 203–212. [CrossRef]
5. Guo, C.X.; Wang, M.; Chen, T.; Lou, X.W.; Li, C.M. A hierarchically nanostructured composite of MnO_2/conjugated polymer/graphene for high-performance lithium ion batteries. *Adv. Energy Mater.* **2011**, *1*, 736–741. [CrossRef]
6. Jo, G.; Choe, M.; Lee, S.; Park, W. The application of graphene as electrodes in electrical and optical devices. *Nanotechnology* **2012**, *23*, 112001. [CrossRef]
7. Hu, W.; Peng, C.; Luo, W.; Lv, M.; Li, X.; Li, D.; Huang, Q.; Fan, C. Graphene-Based Antibacterial Paper. *ACS Nano* **2010**, *4*, 4317–4323. [CrossRef]

8. Kumar, S.; Ojha, A.K.; Patrice, D.; Yadav, B.S.; Materny, A. One step in-situ synthesis of CeO_2 nanoparticles grown on reduced graphene oxide as an excellent fluorescent and photocatalyst material under sunlight irradiation. *Phys. Chem. Chem. Phys.* **2016**, *18*, 11157–11167. [CrossRef] [PubMed]
9. Ghosh, T.K.; Gope, S.; Rana, D.; Roy, I.; Sarkar, G.; Sadhukhan, S.; Bhattacharya, A.; Pramanik, K.; Chattopadhyay, S.; Chakraborty, M.; et al. Physical and electrical characterization of reduced graphene oxide synthesized adopting green route. *Bull. Mater. Sci.* **2016**, *39*, 543–550. [CrossRef]
10. Romero, A.; Lavin-Lopez, M.P.; Sanchez-Silva, L.; Valverde, J.L.; Paton-Carrero, A. Comparative study of different scalable routes to synthesize graphene oxide and reduced graphene oxide. *Mater. Chem. Phys.* **2018**, *203*, 284–292. [CrossRef]
11. Zaaba, N.I.; Foo, K.L.; Hashim, U.; Tan, S.J.; Liu, W.W.; Voon, C.H. Synthesis of Graphene Oxide using Modified Hummers Method: Solvent Influence. *Procedia Eng.* **2017**, *184*, 469–477. [CrossRef]
12. Brodie, B.C. XIII. On the Atomic Weight of Graphite. *Philos. Trans. R. Soc. Lond.* **1859**, *149*, 249–259.
13. Staudenmaier, L. Method for the preparation of the graphite acid. *Eur. J. Inorg. Chem.* **1898**, *31*, 1481–1487.
14. Hummers, W.S.; Offeman, R.E. Preparation of Graphitic Oxide. *J. Am. Chem. Soc.* **1958**, *80*, 1339. [CrossRef]
15. Marcano, D.C.; Kosynkin, D.V.; Berlin, J.M.; Sinitskii, A.; Sun, Z.; Slesarev, A.; Alemany, L.B.; Lu, W.; Tour, J.M. Improved synthesis of graphene oxide. *ACS Nano* **2010**, *4*, 4806–4814. [CrossRef]
16. Smith, A.T.; LaChance, A.M.; Zeng, S.; Liu, B.; Sun, L. Synthesis, properties, and applications of graphene oxide/reduced graphene oxide and their nanocomposites. *Nano Mater. Sci.* **2019**, *1*, 31–47. [CrossRef]
17. Agarwal, V.; Zetterlund, P.B. Strategies for reduction of graphene oxide—A comprehensive review. *Chem. Eng. J.* **2021**, *405*, 127018. [CrossRef]
18. Sharma, N.; Sharma, V.; Jain, Y.; Kumari, M.; Gupta, R.; Sharma, S.K.; Sachdev, K. Synthesis and Characterization of Graphene Oxide (GO) and Reduced Graphene Oxide (rGO) for Gas Sensing Application. *Macromol. Symp.* **2017**, *376*, 1700006. [CrossRef]
19. Longo, A.; Verucchi, R.; Aversa, L.; Tatti, R.; Ambrosio, A.; Orabona, E.; Coscia, U.; Carotenuto, G.; Maddalena, P. Graphene oxide prepared by graphene nanoplatelets and reduced by laser treatment. *Nanotechnology* **2017**, *28*, 224002. [CrossRef]
20. Tran, D.N.H.; Kabiri, S.; Losic, D. A green approach for the reduction of graphene oxide nanosheets using non-aromatic amino acids. *Carbon N. Y.* **2014**, *76*, 193–202. [CrossRef]
21. Azizighannad, S.; Mitra, S. Stepwise reduction of Graphene Oxide (GO) and its effects on chemical and colloidal properties. *Sci. Rep.* **2018**, *8*, 10083. [CrossRef]
22. Stankovich, S.; Dikin, D.A.; Piner, R.D.; Kohlhaas, K.A.; Kleinhammes, A.; Jia, Y.; Wu, Y.; Nguyen, S.B.T.; Ruoff, R.S. Synthesis of graphene-based nanosheets via chemical reduction of exfoliated graphite oxide. *Carbon N. Y.* **2007**, *45*, 1558–1565. [CrossRef]
23. Wang, G.; Yang, J.; Park, J.; Gou, X.; Wang, B.; Liu, H.; Yao, J. Facile Synthesis and characterization of graphene nanosheets. *J. Phys. Chem. C* **2008**, *112*, 8192–8195. [CrossRef]
24. Si, Y.; Samulski, E.T. Synthesis of Water Soluble Graphene 2008. *Nano Lett.* **2008**, *8*, 1679–1682. [CrossRef] [PubMed]
25. Chua, C.K.; Pumera, M. Chemical reduction of graphene oxide: A synthetic chemistry viewpoint. *Chem. Soc. Rev.* **2014**, *43*, 291–312. [CrossRef]
26. Mei, X.; Ouyang, J. Ultrasonication-assisted ultrafast reduction of graphene oxide by zinc powder at room temperature. *Carbon N. Y.* **2011**, *49*, 5389–5397. [CrossRef]
27. Agharkar, M.; Kochrekar, S.; Hidouri, S.; Azeez, M.A. Trends in green reduction of graphene oxides, issues and challenges: A review. *Mater. Res. Bull.* **2014**, *59*, 323–328. [CrossRef]
28. Medha, G.; Sharmila, C.; Anil, G. Green Synthesis and Characterization of Nanocrystalline Graphene Oxide. *Int. Res. J. Sci. Eng.* **2017**, *1*, 29–34.
29. Shubha, P.; Namratha, K.; Aparna, H.S.; Ashok, N.R.; Mustak, M.S.; Chatterjee, J.; Byrappa, K. Facile green reduction of graphene oxide using *Ocimum sanctum* hydroalcoholic extract and evaluation of its cellular toxicity. *Mater. Chem. Phys.* **2017**, *198*, 66–72. [CrossRef]
30. Rice-Evans, C.A.; Miller, N.J.; Paganga, G. Structure-antioxidant activity relationships of flavonoids and phenolic acids. *Free Radic. Biol. Med.* **1996**, *20*, 933–956. [CrossRef]
31. Thakur, S.; Karak, N. Green reduction of graphene oxide by aqueous phytoextracts. *Carbon N. Y.* **2012**, *50*, 5331–5339. [CrossRef]
32. Gurunathan, S.; Han, J.W.; Eppakayala, V.; Dayem, A.A.; Kwon, D.; Kim, J. Biocompatibility effects of biologically synthesized graphene in primary mouse embryonic fibroblast cells. *Nanoscale Res. Lett.* **2013**, *8*, 393. [CrossRef]
33. Gurunathan, S.; Han, J.W.; Park, J.H.; Eppakayala, V.; Kim, J.H. Ginkgo biloba: A natural reducing agent for the synthesis of cytocompatible graphene. *Int. J. Nanomed.* **2014**, *9*, 363–377. [CrossRef] [PubMed]
34. Lalitha, M.J.F.P. Phyto-reduction of graphene oxide using the aqueous extract of *Eichhornia crassipes* (Mart.) Solms. *Int. Nano Lett.* **2014**, *4*, 103–108. [CrossRef]
35. Khan, M.; Al-marri, A.H.; Khan, M.; Mohri, N.; Adil, S.F.; Al-Warthan, A.; Siddiqui, M.R.H.; Alkhathlan, H.Z.; Berger, R.; Tremel, W.; et al. Pulicaria glutinosa plant extract: A green and eco- friendly reducing agent for the preparation of highly reduced graphene oxide. *RSC Adv.* **2014**, *4*, 24119–24125. [CrossRef]
36. Lee, G.; Kim, B.S. Biological reduction of graphene oxide using plant leaf extracts. *Biotechnol. Prog.* **2014**, *30*, 463–469. [CrossRef]
37. Kumar, G.G.; Babu, K.J.; Nahm, K.S.; Hwang, Y.J. A facile one-pot green synthesis of reduced graphene oxide and its composites for non- enzymatic hydrogen peroxide sensor applications. *RSC Adv.* **2014**, *4*, 7944–7951. [CrossRef]

38. Atarod, M.; Nasrollahzadeh, M.; Sajadi, S.M. Green synthesis of a Cu/reduced graphene oxide/ Fe3O4 nanocomposite using *Euphorbia wallichii* leaf extract and its application as a recyclable and heterogeneous catalyst for the reduction of 4- nitrophenol and rhodamine B. *RSC Adv.* **2015**, *5*, 91532–91543. [CrossRef]
39. Jana, M.; Saha, S.; Samanta, P.; Chandra, N.; Hee, J.; Kuila, T. Investigation of the capacitive performance of tobacco solution reduced graphene oxide. *Mater. Chem. Phys.* **2015**, *151*, 72–80. [CrossRef]
40. Suresh, D.; Nethravathi, P.C.; Udayabhanu; Nagabhushana, H.; Sharma, S.C. Spinach assisted green reduction of graphene oxide and its antioxidant and dye absorption properties. *Ceram. Int.* **2015**, *41*, 4810–4813. [CrossRef]
41. Chamoli, P.; Sharma, R.; Das, K.; Kar, K.K. *Mangifera indica*, *Ficus religiosa* and *Polyalthia longifolia* leaf extract-assisted green synthesis of graphene for transparent highly conductive film. *RSC Adv.* **2016**, *6*, 96355–96366. [CrossRef]
42. Chettri, P.; Vendamani, V.S.; Tripathi, A.; Pathak, A.P.; Tiwari, A. Self assembly of functionalised graphene nanostructures by one step reduction of graphene oxide using aqueous extract of Artemisia vulgaris. *Appl. Surf. Sci.* **2016**, *362*, 221–229. [CrossRef]
43. Sadhukhan, S.; Kumar, T.; Rana, D.; Roy, I. Studies on synthesis of reduced graphene oxide (RGO) via green route and its electrical property. *Mater. Res. Bull.* **2016**, *79*, 41–51. [CrossRef]
44. Xing, F.Y.; Guan, L.L.; Li, Y.L.; Jia, C.J. Biosynthesis of reduced graphene oxide nanosheets and their in vitro cytotoxicity against cardiac cell lines of Catla catla. *Environ. Toxicol. Pharmacol.* **2016**, *48*, 110–115. [CrossRef]
45. Baioun, A.; Kellawi, H.; Falah, A. A modified electrode by a facile green preparation of reduced graphene oxide utilizing olive leaves extract. *Carbon Lett.* **2017**, *24*, 47–54. [CrossRef]
46. Elif, Ö.; Belma, Ö.; Ilkay, Ş. Production of biologically safe and mechanically improved reduced graphene oxide/hydroxyapatite composites. *Mater. Res. Express* **2017**, *4*, 015601. [CrossRef]
47. Chandu, B.; Sai, V.; Mosali, S.; Mullamuri, B.; Bollikolla, H.B. A facile green reduction of graphene oxide using *Annona squamosa* leaf extract. *Carbon Lett.* **2017**, *21*, 74–80. [CrossRef]
48. Li, C.; Zhuang, Z.; Jin, X.; Chen, Z. A facile and green preparation of reduced graphene oxide using *Eucalyptus* leaf extract. *Appl. Surf. Sci.* **2017**, *422*, 469–474. [CrossRef]
49. Moosa, A.A.; Jaafar, J.N. Green reduction of graphene oxide using tea leaves extract with applications to lead ions removal from water. *Nanosci. Nanotechnol.* **2017**, *7*, 38–47. [CrossRef]
50. Zhu, X.; Xu, X.; Liu, F.; Jin, J.; Liu, L.; Zhi, Y.; Chen, Z.; Zhou, Z.; Yu, J. Green synthesis of graphene nanosheets and their in vitro cytotoxicity against human prostate cancer (DU 145) cell lines. *Nanomater. Nanotechnol.* **2017**, *7*, 1–7. [CrossRef]
51. Bhattacharya, G.; Sas, S.; Wadhwa, S.; Mathur, A.; McLaughlin, J.; Roy, S.S. Aloe vera assisted facile green synthesis of reduced graphene oxide for electrochemical and dye removal applications. *RSC Adv.* **2017**, *7*, 26680–26688. [CrossRef]
52. Ramanathan, S.; Elanthamilan, E.; Obadiah, A.; Durairaj, A.; Merlin, J.P.; Ramasundaram, S.; Vasanthkumar, S. Aloe vera (L.) Burm f. extract reduced graphene oxide for supercapacitor application. *J. Mater. Sci. Mater. Electron.* **2017**, *28*, 16648–16657. [CrossRef]
53. Mahata, S.; Sahu, A.; Shukla, P.; Rai, A.; Singh, M.; Rai, V.K. Bio-inspired unprecedented synthesis of reduced graphene oxide: Catalytic probe for electro-/chemical reduction of nitro group in aqueous medium. *New J. Chem.* **2018**, *42*, 2067–2073. [CrossRef]
54. Jin, X.; Li, N.; Weng, X.; Li, C.; Chen, Z. Green reduction of graphene oxide using *Eucalyptus* leaf extract and its application to remove dye. *Chemosphere* **2018**, *208*, 417–424. [CrossRef] [PubMed]
55. Mahata, S.; Sahu, A.; Shukla, P.; Rai, A.; Singh, M.; Rai, V.K. The novel and efficient reduction of graphene oxide using *Ocimum sanctum* L. leaf extract as an alternative renewable bio-resource. *New J. Chem.* **2018**, *42*, 19945–19952. [CrossRef]
56. Elemike, E.E.; Onwudiwe, D.C.; Wei, L.; Lou, C.; Zhao, Z. Synthesis of nanostructured ZnO, AgZnO and the composites with reduced graphene oxide (rGO-AgZnO) using leaf extract of *Stigmaphyllon ovatum*. *J. Environ. Chem. Eng.* **2019**, *7*, 103190. [CrossRef]
57. Fahiminia, M.; Shamabadi, N.S.; Nasrollahzadeh, M.; Mohammad Sajadi, S. Phytosynthesis of Cu/rGO using *Euphorbia cheiradenia* Boiss extract and study of its ability in the reduction of organic dyes and 4-nitrophenol in aqueous medium. *IET Nanobiotechnol.* **2019**, *13*, 202–213. [CrossRef] [PubMed]
58. Ghosh, T.K.; Sadhukhan, S.; Rana, D.; Bhattacharyya, A.; Chattopadhyay, D.; Chakraborty, M. Green approaches to synthesize reduced graphene oxide and assessment of its electrical properties. *Nano Struct. Nano Objects* **2019**, *19*, 100362. [CrossRef]
59. Khojasteh, H.; Safajou, H.; Mortazavi-Derazkola, S.; Salavati-Niasari, M.; Heydaryan, K.; Yazdani, M. Economic procedure for facile and eco-friendly reduction of graphene oxide by plant extracts; a comparison and property investigation. *J. Clean. Prod.* **2019**, *229*, 1139–1147. [CrossRef]
60. Lin, Z.; Weng, X.; Ma, L.; Sarkar, B.; Chen, Z. Mechanistic insights into Pb(II) removal from aqueous solution by green reduced graphene oxide. *J. Colloid Interface Sci.* **2019**, *550*, 1–9. [CrossRef]
61. Mahmudzadeh, M.; Yari, H.; Ramezanzadeh, B.; Mahdavian, M. Highly potent radical scavenging-anti-oxidant activity of biologically reduced graphene oxide using Nettle extract as a green bio-genic amines- based reductants source instead of hazardous hydrazine hydrate. *J. Hazard. Mater.* **2019**, *371*, 609–624. [CrossRef] [PubMed]
62. Lin, S.; Ruan, J.; Wang, S. Biosynthesized of reduced graphene oxide nanosheets and its loading with paclitaxel for their anti cancer effect for treatment of lung cancer. *J. Photochem. Photobiol. B Biol.* **2019**, *191*, 13–17. [CrossRef]
63. Veisi, H.; Tamoradi, T.; Karmakar, B.; Mohammadi, P.; Hemmati, S. In situ biogenic synthesis of Pd nanoparticles over reduced graphene oxide by using a plant extract (*Thymbra spicata*) and its catalytic evaluation towards cyanation of aryl halides. *Mater. Sci. Eng. C* **2019**, *104*, 109919. [CrossRef] [PubMed]

64. Lingaraju, K.; Raja Naika, H.; Nagaraju, G.; Nagabhushana, H. Biocompatible synthesis of reduced graphene oxide from *Euphorbia heterophylla* (L.) and their in-vitro cytotoxicity against human cancer cell lines. *Biotechnol. Rep.* **2019**, *24*, e00376. [CrossRef]
65. Wang, C.; Wang, X.; Chen, Y.; Fang, Z. In-vitro photothermal therapy using plant extract polyphenols functionalized graphene sheets for treatment of lung cancer. *J. Photochem. Photobiol. B Biol.* **2020**, *204*, 111587. [CrossRef]
66. Faiz, M.S.A.; Azurahanim, C.A.C.; Raba, S.A.; Ruzniza, M.Z. Low Cost and Green Approach in The Reduction of Graphene Oxide (GO) Using Palm Oil Leaves Extract for Potential in Industrial Applications. *Results Phys.* **2020**, *16*, 102954. [CrossRef]
67. Sabayan, B.; Goudarzian, N.; Moslemin, M.H.; Mohebat, R. Green synthesis and high efficacy method for reduced graphene oxide by *Zataria multiflora* extract. *J. Environ. Treat. Tech.* **2020**, *8*, 488–496.
68. Olorunkosebi, A.A.; Eleruja, M.A.; Adedeji, A.V.; Olofinjana, B.; Fasakin, O.; Omotoso, E.; Oyedotun, K.O.; Ajayi, E.O.B.; Manyala, N. Optimization of graphene oxide through various Hummers' methods and comparative reduction using green approach. *Diam. Relat. Mater.* **2021**, *117*, 108456. [CrossRef]
69. Parthipan, P.; Al-Dosary, M.A.; Al-Ghamdi, A.A.; Subramania, A. Eco-friendly synthesis of reduced graphene oxide as sustainable photocatalyst for removal of hazardous organic dyes. *J. King Saud Univ. Sci.* **2021**, *33*, 101438. [CrossRef]
70. Andrianiaina, H.; Razanamahandry, L.C.; Sackey, J.; Ndimba, R.; Khamlich, S.; Maaza, M. Synthesis of graphene sheets from graphite flake mediated with extracts of various indigenous plants from Madagascar. *Mater. Today Proc.* **2021**, *36*, 553–558. [CrossRef]
71. Punniyakotti, P.; Aruliah, R.; Angaiah, S. Facile synthesis of reduced graphene oxide using *Acalypha indica* and *Raphanus sativus* extracts and their in vitro cytotoxicity activity against human breast (MCF-7) and lung (A549) cancer cell lines. *3 Biotech* **2021**, *11*, 157. [CrossRef] [PubMed]
72. Qi, J.; Zhang, S.; Xie, C.; Liu, Q.; Yang, S. Fabrication of *Erythrina senegalensis* leaf extract mediated reduced graphene oxide for cardiac repair applications in the nursing care. *Inorg. Nano Metal Chem.* **2021**, *51*, 143–149. [CrossRef]
73. Jha, P.K.; Khongnakorn, W.; Chawenjkigwanich, C.; Chowdhury, M.S.; Techato, K. Eco-friendly reduced graphene oxide nanofilter preparation and application for iron removal. *Separations* **2021**, *8*, 68. [CrossRef]
74. Kartick, B.; Srivastava, S.K.; Srivastava, I. Green Synthesis of Graphene. *J. Nanosci. Nanotechnol.* **2013**, *13*, 4320–4324. [CrossRef] [PubMed]
75. Tavakoli, F.; Salavati-Niasari, M.; Badiei, A.; Mohandes, F. Green synthesis and characterization of graphene nanosheets. *Mater. Res. Bull.* **2015**, *63*, 51–57. [CrossRef]
76. Upadhyay, R.K.; Soin, N.; Saha, S.; Barman, A.; Roy, S.S. Grape extract assisted green synthesis of reduced graphene oxide for water treatment application. *Mater. Lett.* **2015**, *160*, 355–358. [CrossRef]
77. Maddinedi, S.B.; Mandal, B.K. Biofabrication of Reduced Graphene Oxide Nanosheets Using *Terminalia bellirica* Fruit Extract. *Curr. Nanosci.* **2016**, *12*, 94–102. [CrossRef]
78. Hou, D.; Liu, Q.; Cheng, H.; Li, K. Graphene Synthesis via Chemical Reduction of Graphene Oxide Using Lemon Extract. *J. Nanosci. Nanotechnol.* **2017**, *17*, 6518–6523. [CrossRef]
79. Hou, D.; Liu, Q.; Cheng, H.; Zhang, H.; Wang, S. Green reduction of graphene oxide via Lycium barbarum extract. *J. Solid State Chem.* **2017**, *246*, 351–356. [CrossRef]
80. Ansari, M.Z.; Siddiqui, W.A. Deoxygenation of graphene oxide using biocompatible reducing agent *Ficus carica* (dried ripe fig). *J. Nanostructure Chem.* **2018**, *8*, 431–440. [CrossRef]
81. Ansari, M.Z.; Lone, M.N.; Sajid, S.; Siddiqui, W.A. Novel Green Synthesis of Graphene Layers using Zante Currants and Graphene Oxide. *Orient. J. Chem.* **2018**, *34*, 2832–2837. [CrossRef]
82. Ansari, M.Z.; Rahul, J.; Siddiqui, W.A. Novel and green synthesis of chemically reduced graphene sheets using *Phyllanthus emblica* (Indian Gooseberry) and its photovoltaic activity. *Mater. Res. Express* **2019**, *6*, 055027. [CrossRef]
83. Raja, A.; Rajasekaran, P.; Selvakumar, K.; Arivanandhan, M.; Asath Bahadur, S.; Swaminathan, M. Green approach to the preparation of reduced graphene oxide for photocatalytic and supercapacitor application. *Optik* **2019**, *190*, 21–27. [CrossRef]
84. Parthipan, P.; Cheng, L.; Rajasekar, A.; Govarthanan, M.; Subramania, A. Biologically reduced graphene oxide as a green and easily available photocatalyst for degradation of organic dyes. *Environ. Res.* **2021**, *196*, 110983. [CrossRef] [PubMed]
85. Panicker, N.J.; Sahu, P.P. Green reduction of graphene oxide using phytochemicals extracted from *Pomelo grandis* and *Tamarindus indica* and its supercapacitor applications. *J. Mater. Sci. Mater. Electron.* **2021**, *32*, 15265–15278. [CrossRef]
86. Smina, C.S.; Lalitha, P.; Sharma, S.C.; Nagabhushana, H. Screening of anti-cancer activity of reduced graphene oxide biogenically synthesized against human breast cancer MCF-7 cell lines. *Appl. Nanosci.* **2021**, *11*, 1093–1105. [CrossRef]
87. Haghighi, B.; Tabrizi, M.A. Green-synthesis of reduced graphene oxide nanosheets using rose water and a survey on their characteristics and applications. *RSC Adv.* **2013**, *3*, 13365–13371. [CrossRef]
88. Chu, H.; Lee, C.; Tai, N. Green reduction of graphene oxide by *Hibiscus sabdariffa* L. to fabricate flexible graphene electrode. *Carbon N. Y.* **2014**, *80*, 725–733. [CrossRef]
89. Suresh, D.; Udayabhanu; Nagabhushana, H.; Sharma, S.C. Clove extract mediated facile green reduction of graphene oxide, its dye elimination and antioxidant properties. *Mater. Lett.* **2015**, *142*, 4–6. [CrossRef]
90. Hou, D.; Liu, Q.; Cheng, H.; Li, K.; Wang, D.; Zhang, H. Chrysanthemum extract assisted green reduction of graphene oxide. *Mater. Chem. Phys.* **2016**, *183*, 76–82. [CrossRef]
91. Shahane, S.; Sidhaye, D. Facile biosynthesis of reduced graphene oxide nanostructures via reduction by tagetes erecta (marigold flower) plant extract. *Int. J. Mod. Phys. B* **2018**, *32*, 1840068. [CrossRef]

92. Li, B.; Jin, X.; Lin, J.; Chen, Z. Green reduction of graphene oxide by sugarcane bagasse extract and its application for the removal of cadmium in aqueous solution. *J. Clean. Prod.* **2018**, *189*, 128–134. [CrossRef]
93. Wijaya, R.; Andersan, G.; Santoso, S.P.; Irawaty, W. Green Reduction of Graphene Oxide using Kaffir Lime Peel Extract (*Citrus hystrix*) and Its Application as Adsorbent for Methylene Blue. *Sci. Rep.* **2020**, *10*, 667. [CrossRef]
94. Suresh, D.; Udayabhanu; Kumar, P.M.; Nagabhushana, H.; Sharma, S.C. Cinnamon supported facile green reduction of graphene oxide, its dye elimination and antioxidant activities. *Mater. Lett.* **2015**, *151*, 93–95. [CrossRef]
95. Han, W.; Niu, W.; Sun, B.; Shi, G.; Cui, X. Biofabrication of polyphenols stabilized reduced graphene oxide and its anti-tuberculosis activity. *J. Photochem. Photobiol. B Biol.* **2016**, *165*, 305–309. [CrossRef]
96. Singh, A.; Ahmed, B.; Singh, A.; Ojha, A.K. Photodegradation of phenanthrene catalyzed by rGO sheets and disk like structures synthesized using sugar cane juice as a reducing agent. *Spectrochim. Acta Part A Mol. Biomol. Spectrosc.* **2018**, *204*, 603–610. [CrossRef] [PubMed]
97. Ghosh, S.; Das, P.; Baskey, M. Plant extract assisted synthesis of reduced graphene oxide sheet and the photocatalytic performances on cationic and anionic dyes to decontaminate wastewater. *Adv. Nat. Sci. Nanosci. Nanotechnol.* **2021**, *12*, 015008. [CrossRef]
98. Jana, M.; Saha, S.; Khanra, P.; Chandra, N.; Kumar, S.; Kuila, T.; Hee, J. Bio-reduction of graphene oxide using drained water from soaked mung beans (*Phaseolus aureus* L.) and its application as energy storage electrode material. *Mater. Sci. Eng. B* **2014**, *186*, 33–40. [CrossRef]
99. Maddinedi, S.B.; Mandal, B.K.; Vankayala, R.; Kalluru, P.; Pamanji, S.R. Bioinspired reduced graphene oxide nanosheets using Terminalia chebula seeds extract. *Spectrochim. Acta Part A Mol. Biomol. Spectrosc.* **2015**, *145*, 117–124. [CrossRef]
100. Chu, H.; Lee, C.; Tai, N. Green preparation using black soybeans extract for graphene-based porous electrodes and their applications in supercapacitors. *J. Power Sources* **2016**, *322*, 31–39. [CrossRef]
101. Yaragalla, S.; Rajendran, R.; Jose, J.; Almaadeed, M.A.; Kalarikkal, N.; Thomas, S. Preparation and characterization of green graphene using grape seed extract for bioapplications. *Mater. Sci. Eng. C* **2016**, *65*, 345–353. [CrossRef] [PubMed]
102. Tayade, U.S.; Borse, A.U.; Meshram, J.S. Green reduction of graphene oxide and its applications in band gap calculation and antioxidant activity. *Green Mater.* **2019**, *7*, 143–155. [CrossRef]
103. Kuila, T.; Bose, S.; Khanra, P.; Mishra, A.K.; Kim, N.H.; Lee, J.H. A green approach for the reduction of graphene oxide by wild carrot root. *Carbon N. Y.* **2012**, *50*, 914–921. [CrossRef]
104. Akhavan, O.; Ghaderi, E.; Abouei, E.; Hatamie, S.; Ghasemi, E. Accelerated differentiation of neural stem cells into neurons on ginseng-reduced graphene oxide sheets. *Carbon N. Y.* **2013**, *66*, 395–406. [CrossRef]
105. Vusa, C.S.R.; Berchmans, S.; Alwarappan, S. Facile and green synthesis of graphene. *RSC Adv.* **2014**, *4*, 22470–22475. [CrossRef]
106. Khan, M.; Al-marri, A.H.; Khan, M.; Shaik, M.R.; Mohri, N.; Adil, S.F.; Kuniyil, M.; Alkhathlan, H.Z.; Al-warthan, A.; Tremel, W.; et al. Green Approach for the Effective Reduction of Graphene Oxide Using *Salvadora persica* L. Root (Miswak) Extract. *Nanoscale Res. Lett.* **2015**, *10*, 281. [CrossRef]
107. Thongpool, V.; Phunpheok, A.; Piriyawong, V.; Limsuwan, S. Green Approach for the Reduction of Graphene Oxide by Thai Shallot. *Key Eng. Mater.* **2016**, *675–676*, 696–699. [CrossRef]
108. Khanam, P.N.; Hasan, A. Biosynthesis and characterization of graphene by using non-toxic reducing agent from *Allium cepa* extract: Anti-bacterial properties. *Int. J. Biol. Macromol.* **2019**, *126*, 151–158. [CrossRef]
109. Rai, S.; Bhujel, R.; Biswas, J.; Swain, B.P. Biocompatible synthesis of rGO from ginger extract as a green reducing agent and its supercapacitor application. *Bull. Mater. Sci.* **2021**, *44*, 40. [CrossRef]
110. Rahman, O.S.A.; Chellasamy, V.; Ponpandian, N.; Amirthapandian, S.; Panigrahi, B.K.; Thangadurai, P. A facile green synthesis of reduced graphene oxide by using pollen grains of *Peltophorum pterocarpum* and study of its electrochemical behavior. *RSC Adv.* **2014**, *4*, 56910–56917. [CrossRef]
111. Paredes, J.I.; Villar-Rodil, S.; Martínez-Alonso, A.; Tascón, J.M.D. Graphene oxide dispersions in organic solvents. *Langmuir* **2008**, *24*, 10560–10564. [CrossRef] [PubMed]
112. Zhang, T.Y.; Zhang, D. Aqueous colloids of graphene oxide nanosheets by exfoliation of graphite oxide without ultrasonication. *Bull. Mater. Sci.* **2011**, *34*, 25–28. [CrossRef]
113. Aunkor, M.T.; Mahbubul, I.; Saidur, R.; Metselaar, H.S. The green reduction of graphene oxide. *RSC* **2016**, *6*, 27807–27828. [CrossRef]
114. Bosch-navarro, C.; Coronado, E.; Mart-Gastaldo, C.; Sanchez-Royo, J.F.; Gomez, M.G. Influence of the pH on the synthesis of reduced graphene oxide under hydrothermal conditions. *Nanoscale* **2012**, *4*, 3977–3982. [CrossRef]
115. Gotoh, Y.; Hiraiwa, K.; Nagayama, M. In vitro mineralization of osteoblastic cells derived from human bone. *Bone Miner.* **1990**, *8*, 239–250. [CrossRef]